Received: July 6, 2022. Revised: July 30, 2022.

International Journal of
Intelligent Engineering & Systems

http://www.inass.org/

Friction Compensated Force Control of Electro-Hydraulic System Using Fuzzy Controller

Weerapong Chanbua[1]* **Unnat Pinsopon[1]**

[1]*School of Engineering, King Mongkut's Institute of Technology Ladkrabang, Bangkok, Thailand*
* Corresponding author's Email: wrp.chanbua@gmail.com

Abstract: Steady state and dynamic LuGre friction models of an electro-hydraulic system were constructed. Indirect electro-hydraulic cylinder force control under friction compensated PID and fuzzy controllers were tested and compared. Feedback force signal was indirectly measured and calculated from pressures to emulate the applications that direct force measurement is impossible. Estimated friction was compensated to desired force command of the PID controller. The proposed fuzzy controller contained two modules. The first, as a friction compensator, calculated modified error according to estimated friction and feedback force error. The second module calculated control action based on PD control scheme. Friction compensated PID and fuzzy controllers could reduce tracking errors at the maximum force commands by 80% and 90%, respectively, compared to the PID controller without compensation. The steady state friction compensation yielded better tracking performances compared to the dynamic friction. Tracking performance of the fuzzy controller was always better than the PID controller.

Keywords: Electro-hydraulic system, Fuzzy controller, Friction compensation, Indirect force measurement.

1. Introduction

Electro-hydraulic system (EHS) is the mostly used transmission system in heavy-duty applications due to its advantages over other transmission types such as: high power-to-weight ratio, high stiffness and robustness to harsh working conditions. The operation of EHS could be under position, velocity, or force control. The difficulty in controlling EHS is caused by the system nonlinear phenomena such as compressibility, deadband, leakage and friction. Direct measurements of position and velocity in a motion control system could be easily done by various types of sensors. Direct force measurement with the use of force sensor in EHS is however conducted in laboratory level or sophisticated apparatus. It is not practical in all EHS applications especially ones with harsh working conditions. Indirect force measurement with the use of pressure sensor could be usually found in such applications.

The articles [1-2] presented component enhancement for the improvement of EHS force control performance. Pressure relief valve was controlled in accordance with the flow servo valve in the PD-Fuzzy force control of a hydraulic vertical press machine [1]. High volumetric expansion hoses were proposed to replace rigid pipes in the force control of a hydraulic cylinder in order to increase the hydraulic compliance [2]. Model predictive control (MPC) was applied to the force control of an electro-hydraulic servo system [3, 4]. The performance of MPC depends largely on the accuracy of the system modelling. It was stated in [3] that MPC alone yielded similar performance to the PI controller, however it yielded better performance when used in hybrid with the PI controller. While in [4], MPC was claimed to be superior to both PID and fractional order PID controllers. A feedforward force compensation was designed based on the nonlinear EHS model to theoretically discard the force tracking error, and added to the feedback PID force control loop of an electro-hydraulic servo valve-controlled cylinder integrated unit [5]. The experimental tracking error of the PID controller with feedforward compensation though was not reduced to zero because of modeling simplification, was significantly less than that of the

PID controller alone [5]. Neural network was used to construct an inverse EHS model which gave the desired valve spool position according to the desired force [6]. The valve spool position was then controlled by using feedback PD control plus valve feedforward action, and yielded better performance compared to the conventional controllers. Although the use of neural network did not require accurate system modeling as needed in [3-5], it required expertise in the design and training of the network.

The feedback force in [3-6] was directly measured by force transducer. The influence of friction would then be insignificant since the controller perceived the actual force and would try its best to have the actual force tracking the desired force command. The influence of friction would be significant in the case that actual force on load is concerned, but indirect force measurement such as pressure-calculated force is only available. The feedback force signal calculated from cylinder pressures was used in joint torque PI control of an excavator [7]. Friction was neglected in the study, and the pressure-calculated force was assumed to be the actual force on load [7]. Other than the earth moving equipment application, press machine is the other real-world application that utilizes indirect pressure-calculated force measurement. The topic of indirect force measurement has also been being investigated in machine tools applications [8-10]. The article [8] presented the evaluation of grinding force of a cylindrical grinding machine using various regression models whose inputs were the spindle current and other process parameters. The cutting force of a milling machine was predicted using the values of spindle current and/or spindle accelerations depending on the frequency of the cutting process [9]. Spindle current, spindle speed and kinematics information of each axis were used as inputs for the training of a long short-term memory neural network to estimate the process force of a five-axis milling center [10].

Indirect force measurement would be conducted in this study. The motive is to emulate the harsh working condition application cases that direct force measurement could not be implemented. The feedback force signal applied to the force control system in this study would be calculated by using cylinder pressures. With the use of indirect force measurement, effect of friction could not be overlooked. Friction affects the system performance, no matter the system is under position, velocity or force control. The mostly used method to counteract friction problems was to implement a model-based friction compensation [10-17] because of its less complexity compared to friction model-free compensation method. Implementing of a steady state friction compensation is straight forward and was effectively implemented in various applications [10-13]. In the neural network training process of the five-axis milling center process force estimation, friction on each axis of the machine was estimated by Stribeck friction model with the use of velocity data on that axis [10]. Stribeck friction model was used to estimate the friction at a hydraulic cylinder of an excavator [11]. The estimated friction and load force were used as inputs for feedforward compensation to the displacement command, and the feedforward outperformed the PID controller in displacement tracking [11]. The experiments in [11] were done under a constant known load force, therefore an accurate load force measurement is needed to guarantee its successful implementation in real-world applications. A proposed reaction observer consisted of a disturbance observer working in combination with compensations of static friction, backlash and oil leakage, could effectively estimate reaction force acting on a hydraulic actuator [12]. Steady state friction model of a flexible robot joint was constructed by curve fitting of piecewise continuous polynomial functions, and robot joint velocity control performance was improved with the friction compensation in the PI controller compared to the controller without compensation [13].

Unlike static model, dynamic friction model requires extra efforts in both model identification and implementation. LuGre dynamic friction model has gained popularity among scholars recently [14-17]. The article [14] explored the effectiveness of four different friction models. LuGre friction model was found to be the most versatile, yet its parameter identification was the most complicated [14]. A systematic approach of experimentally evaluating LuGre friction model parameters was proposed [15]. The dynamic LuGre friction was compensated to the PI controller and significantly improved the position control performance of a CNC machine compared to the controller without compensation [15]. Implementing an observer based on the LuGre friction model is an alternative approach to estimate dynamic friction [16, 17]. Multiple-surface sliding (MSS) controller in combination with a dynamic LuGre friction compensation achieved a better performance in position control of a pneumatic actuator compared to the MSS controller alone [16]. A double observer for the estimation of LuGre friction was proposed, and the friction compensation was added to a robust controller in the position control of a digital hydraulic cylinder system [17]. Simulation results presented better performance of

Received: July 6, 2022. Revised: July 30, 2022.

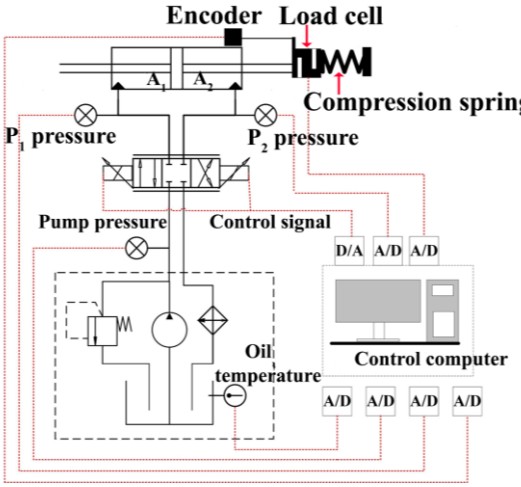

Figure. 1 Schematic diagram of the EHS setup used in this study

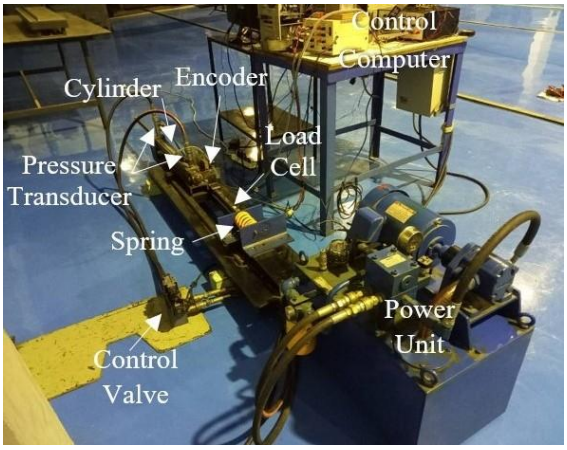

Figure. 2 Experimental test rig

the proposed system compared to the PID controller, similar to [11] the proposed system required an accurate measurement of load force in actual application.

In addition to the selection of friction model, choice of controller to be used in combination with friction compensation is also important. Fuzzy controller imitates human decision making and can deal with complex problems. The controller which was proved to be simple to implement yet powerful, has been effectively implemented in various applications that dealt with nonlinearities [18-20]. The performance of a fuzzy controller was better than PID and genetic algorithm controllers on a cruise control application [18]. Fuzzy control yielded a better transient performance compared to PID controller in a 6 DOF robot manipulator joint control system, though both controllers gave the same converged steady state response [19]. Fuzzy control, implemented along with a simple static friction compensation, could control pneumatic cylinder position to a sub-micrometers order accuracy [20].

This paper presents a practical approach to enhance the force tracking capability of the indirect force control EHS applications. While indirect pressure-calculated force would be used as the feedback force signal, the tracking performance would be judged with the cylinder actual force directly measured by a load cell transducer. Steady state and Dynamic LuGre friction models of EHS would be investigated and constructed using indirect force measurements. Two types of controllers would be studied and compared. A conventional PID controller was used as the benchmark. The other is fuzzy controller which was proved its ability in dealing with system nonlinearity. Both estimated steady state and dynamic frictions would be compensated to both PID and fuzzy controllers, and their effectiveness would be extensively compared. Performance criteria for comparing controllers were the tracking error at the maximum force command and the RMS tracking error. Tracking error considered in the criteria was the difference between the force command and directly measured cylinder force, not the pressure-calculated feedback force.

The organization of the rest of the paper is as follows. Section 2 provides the information of the experimental test setup used in this study. Construction of LuGre friction model of the EHS cylinder system is explained in section 3. Details of the controllers used in this study are described in section 4. Experimental results are discussed in section 5, and the conclusions are drawn in section 6.

2. Electro-hydraulic control system

Fig. 1 shows the diagram of the EHS setup used in this study. Hydraulic oil flow was supplied by a gear pump. The cylinder used in this study was a double-rod type. The piston areas of both ends of the cylinder are equal, $A_1 = A_2 = A$. The data that were measured and sent to the control computer via A/D ports included piston-rod displacement, cylinder force, oil pressures at both ends of the cylinder, pump pressure and oil temperature. The control action was calculated on the computer, and output via D/A port to the proportional directional control valve. To minimize the influence of oil viscosity on the friction, oil temperature was kept between 40-50 □C during conducting all the tests. A compression spring with a spring constant changing between 180 to 220 kN/m according to the compressed length was used to emulate the external load for the cylinder. The feedback cylinder force signal used in this study was calculated according to oil pressures measured at both ends, and is equal to $(P_1-P_2)\cdot A$. The cylinder

Received: July 6, 2022. Revised: July 30, 2022.

Table 1. The specifications of EHS components

Hydraulic gear pump Manufacturer: Volumetric displacement:	 Honor 2GG1U11R 11 cc/rev
Directional control valve Manufacturer: Type:	 Tokimec COM-3-2C-AN-11 4/3 proportional, closed center
Double-rod cylinder Bore / Rod: Stroke:	 0.04 m / 0.028 m 0.50 m
Encoder Manufacturer: Resolution:	 Omron E6B2-CW6C 1,000 pulses/rev
Pressure transducer Manufacturer: Type:	 Wika A-10 piezo-electric type, 0-400 bar
Load cell Manufacturer: Type:	 Zega Keed S-type, 500 kg

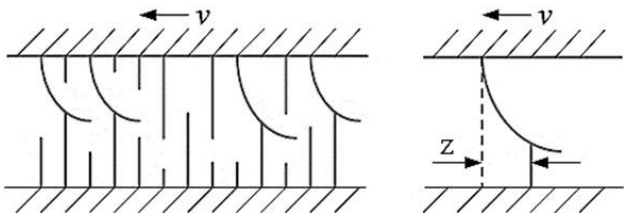

Figure. 3 Bristle behavior of friction between 2 surfaces

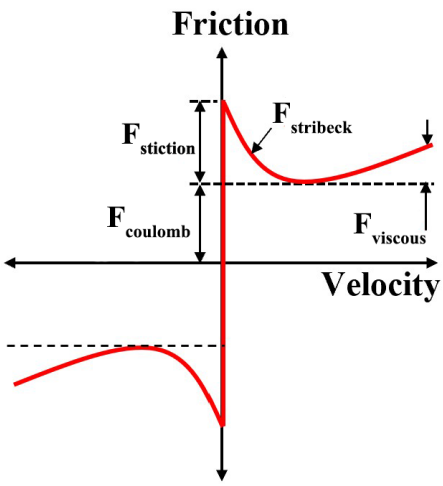

Figure. 4 Characteristics of steady state friction

force sensed by the load cell transducer was only used for verification. The specifications of the major components of the experimental setup are shown in Table 1. Fig. 2 shows the picture of the EHS experimental test rig used in this study.

3. Modeling of hydraulic cylinder friction

3.1 LuGre friction model

For a concise manuscript, the description of LuGre frinction model would be briefly explained as follows. The explanation of the model in great details could be found in [21]. The friction between two surfaces is mimicked by the spring-damper characteristics of bristle deflection as shown in Fig. 3. The average deflection of bristles is denoted by z. The time derivative of the average bristle deflection could be explained by the Eq. (1) where ν is the relative velocity of the two surfaces, and α_0 is the bristle stiffness. The Stribeck function, g(ν), is expressed by Eq. (2). The value of g(ν) depends on the material property, surface lubrication and temperature. F_c is the Coulomb friction, F_s is the stiction friction, and ν_s is the Stribeck velocity.

$$\frac{dz}{dt} = v - \alpha_0 \frac{|v|}{g(v)} z \tag{1}$$

$$g(v) = F_C + (F_S - F_C)e^{-\left(\frac{v}{v_S}\right)^2} \tag{2}$$

Friction is large at the beginning of the motion, and its value decreases as the motion proceeds. Friction according to the bristle model could be calculated by Eq. (3), where α_1 is the damping coefficient of the bristle. Adding the influence of the viscosity of the surface contact, LuGre friction model is finally obtained. LuGre friction could be calculated by Eq. (4), where α_2 is the viscous damping coefficient of the surface contact.

$$F_{friction,Bristle} = \alpha_0 z + \alpha_1 \frac{dz}{dt} \tag{3}$$

$$F_{friction,Lugre} = \alpha_0 z + \alpha_1 \frac{dz}{dt} + \alpha_2 v \tag{4}$$

Considering the model at the steady state, the time derivative of z is zero, and the bristle steady state deflection (z_{ss}) is shown by Eq. (5). Substituting z_{ss} into Eq. (4), steady state friction (F_{ss}) which depends only the velocity could then be expressed as Eq. (6). The characteristics of steady state friction could be graphically depicted as Fig. 4.

$$z_{SS} = \frac{sign(v)}{\alpha_0} g(v) \tag{5}$$

$$F_{SS} = F_C + (F_S - F_C)e^{-\left(\frac{v}{v_S}\right)^2} + \alpha_2 v \tag{6}$$

3.2 Evaluation of friction model parameters

Friction in the EHS cylinder could be directly calculated from force balance on the cylinder piston as expressed by Eq. (7), where $F_{friction}$ is friction force, P_1 and P_2 are the oil pressure at the oil-incoming cylinder end, A is piston area, m is piston mass and a

Received: July 6, 2022. Revised: July 30, 2022.

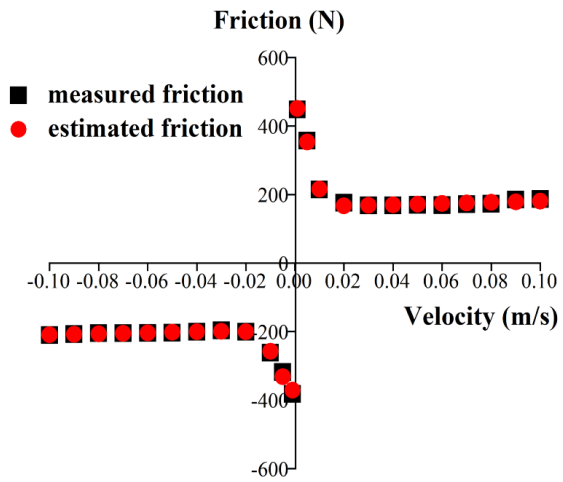

Figure. 5 Comparison of estimated steady state frictions and measured frictions at various constant velocities

Table 2. The Parameters of LuGre friction model.

Parameter	Positive velocity	Negative velocity
F_c (N)	163.152	-194.730
F_s (N)	456.037	-372.657
v_s (m/s)	0.00756	-0.00966
α_0 (Ns/m)	2,000,000	600,000
α_1 (Ns/m)	1,000	1,000
α2 (Ns/m)	175.202	145.923

is piston acceleration. Note that the friction calculated by Eq. (7) was obtained without the direct measurement of cylinder force. The LuGre model parameters were experimentally evaluated based on the guideline described in the article [15]. First, steady state parameters were evaluated. Cylinder piston was controlled to follow various constant velocity commands ranging between -0.10 and 0.10 m/s. The actual frictions occurred during the tests were calculated by Eq. (7). Nonlinear generalization reduced gradient fitting technique was used to determine the values of the parameters, F_c, F_s and α_2 of the steady state friction model (Eq. (6)). The values of the steady state parameters are shown in Table 2. Fig. 5 shows the plots of frictions at various velocities obtained from the calculation of steady state friction model versus the values obtained from the tests.

$$F_{friction} = (P_1 - P_2)A - ma \qquad (7)$$

To evaluate the values of the dynamic LuGre model parameters, the hydraulic cylinder was controlled to move at various constant accelerations ranging from 0.001 to 0.1 m/s^2 for positive motion, and -0.1 to -0.001 m/s^2 for negative motion. The dynamic model was integrated with the values of the parameters α_0 and α_1 picked by trial and error. The values of calculated frictions were compared to ones

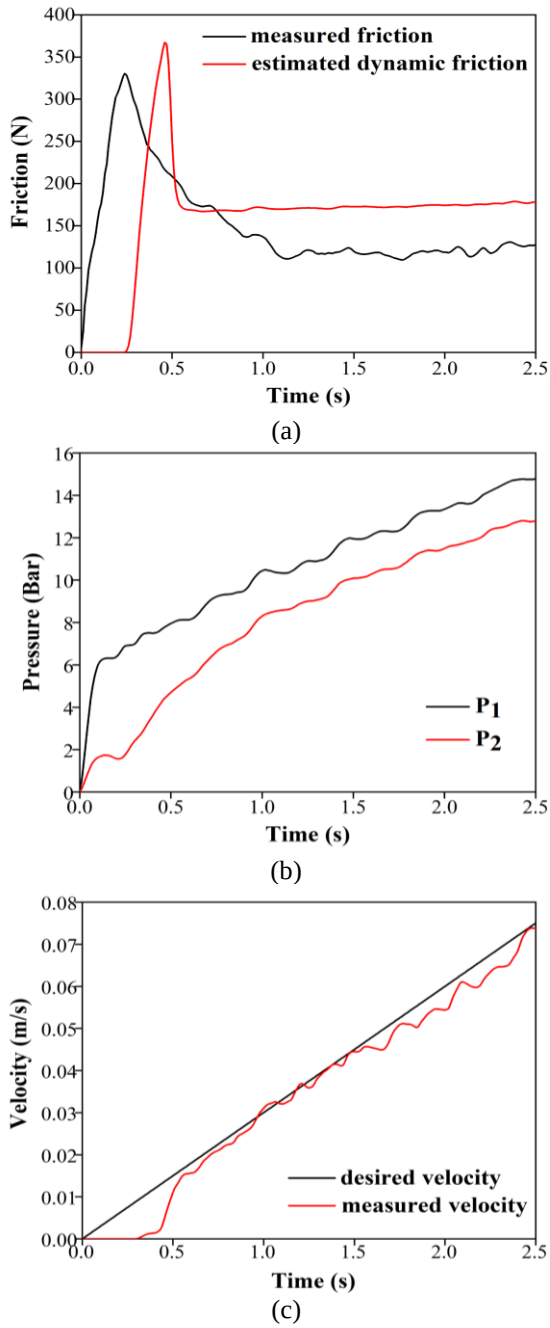

Figure. 6 Calculation of dynamic friction of 0.03 m/s^2 acceleration positive motion case: (a) Calculated dynamic friction, (b) Pressures at both cylinder ends and (c) Cylinder piston velocity

obtained from the tests. The values of the parameters of the dynamic model are also shown in Table 2. Note that the values of the parameters of both steady state and dynamic models were obtained differently for the cases of positive and negative motions.

To show the accuracy of the dynamic model, the frictions obtained from the calculation versus the measured frictions from the tests are selectively shown in Fig. 6 and 7. Fig. 6 shows the result from a positive motion case with the acceleration of 0.03

Received: July 6, 2022. Revised: July 30, 2022.

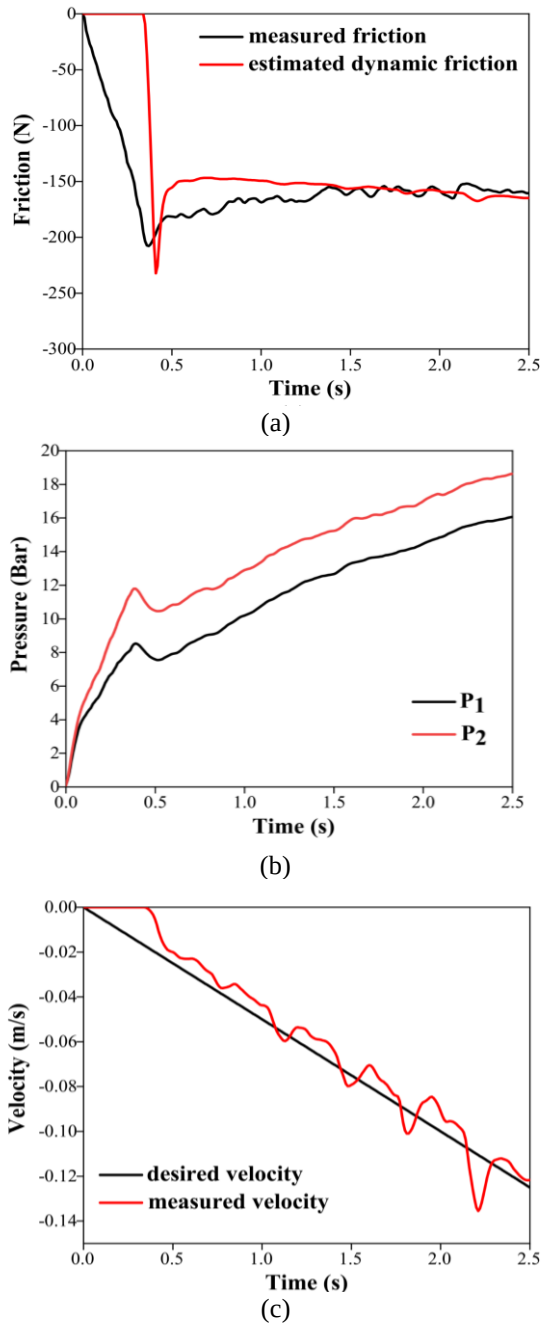

Figure. 7 Calculation of dynamic friction of 0.05 m/s^2 deceleration negative motion case: (a) Calculated dynamic friction, (b) Pressures at both cylinder ends and (c) Cylinder piston velocity

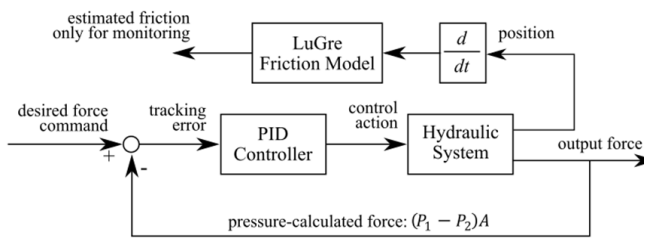

Figure. 8 Block diagram of the PID controller used in the preliminary test

m/s^2, while Fig. 7 shows the result from a negative motion case with the deceleration of -0.05 m/s^2. Due to stiction friction, the cylinder did not move until the time around 0.25 second for the positive motion case (Fig. 6 (c)). The calculated friction which depends solely on the velocity (Eqs. (1)-(4)) therefore remained zero during the first 0.25 second (Fig. 6(a)). This stiction caused the compression of hydraulic oil. The oil pressure at the oil-incoming cylinder end P_1, came to its first peak at the time 0.25 second and its value dropped after the time 0.25 second since the oil expanded once the piston started to move (Fig. 6(b)). The maximum value of estimated friction was about 15% higher than the measured one, and its peak was delayed by roughly 0.25 second. Same trend could be observed for the cylinder negative motion case as seen in Fig. 7, except that the negative motion started at the time slightly before 0.5 second, and P_2 is the oil pressure at the oil-incoming cylinder end.

3.3 Influence of friction on an EHS force control system

Fig. 8 shows the block diagram of the PID force control system used in a preliminary test to show the influence of friction on the EHS force control. As mentioned earlier, the feedback force signal was calculated using cylinder pressures. Both steady state and dynamic LuGre friction models were used to estimate the friction in the cylinder. Fig. 9 (a) shows both the pressure-calculated force response as well as the actual force response sensed by the load cell transducer. Fig. 9 (b) shows estimated frictions from both steady state and dynamic models as well as measured friction calculated by Eq. (7). The calculated feedback force followed the desired force command well. However, when considering the actual force measured by load cell, a 500.71 N tracking error could be observed at the maximum force command. This is due to the friction that the feedback pressure-calculated force signal did not perceive.

During the minimum and maximum force holdings, the piston velocity was roughly zero, the values estimated steady state frictions swayed between its maximum positive and negative values. The noise of the differentiated velocity signal around the zero velocity was the cause for the estimation of swaying frictions. The dynamic LuGRE friction model, with the need of integration, gave a much cleaner estimation of friction compared to the static model. Using pressure-calculated force as a feedback signal, the linear PID controller did not cope well with friction in a hydraulic cylinder. Large tracking

Received: July 6, 2022. Revised: July 30, 2022.

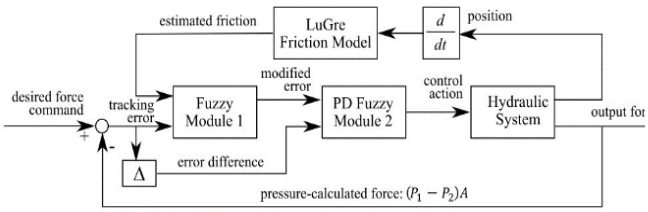

Figure. 11 Fuzzy control with friction compensation block diagram

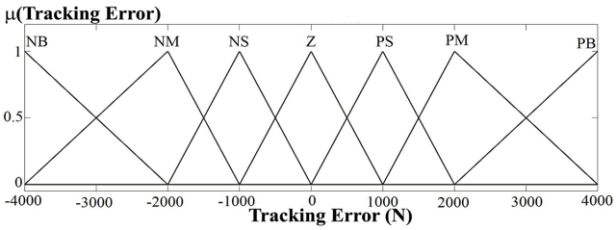

(a)

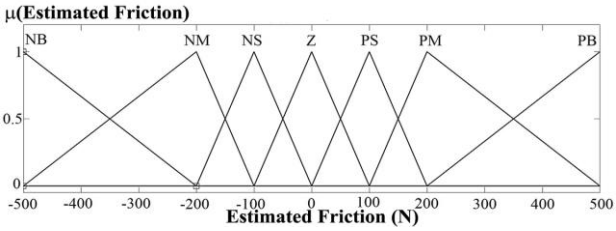

(b)

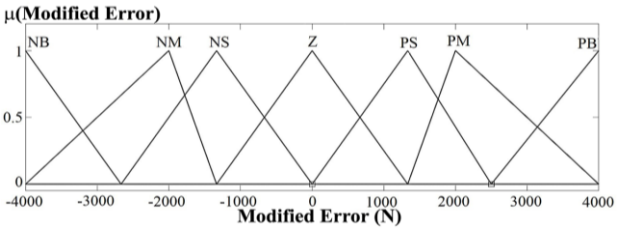

(c)

Figure. 12 Membership functions of fuzzy Control module 1: (a) tracking error input, (b) estimated friction input and (c) modified error output

error at the maximum force command could not be avoided. Stiction friction also caused large delay in actual force at the beginning of direction-changing motion.

4. Controller designs

The performances of two different controllers, PID and fuzzy controllers, were compared in this study. Friction compensation would be applied to both controllers. The conventional PID was used as the benchmark. Fuzzy controller, with its ability of dealing with nonlinear phenomena, would be utilized as an alternative controller with the hope that it could ease the friction problem.

4.1 Friction compensated PID controller

A standard linear PID controller with friction compensation was used in this study (Fig. 10). Friction compensation is done by adding the LuGre estimated friction to the desired force command. The effectiveness of both estimated steady state and dynamic frictions on the PID controller would be tested and compared. The PID control action, u_{PID}, is calculated by Eq. (8), where K_p, K_I, K_D are the gain for the proportional, integral and derivative terms, respectively.

As mentioned earlier, the feedback tracking error, e(t), is the difference between compensated desired force command and pressure-calculated force. The gains K_P K_I K_D were experimentally tuned by the Ziegler–Nichols method. The performance of the PID controller depends largely on the accuracy of the friction estimation. The fact that feedback pressure-calculated force could track the compensated desired force well does not guarantee the good tracking of actual force unless the friction estimation is accurate (Fig. 9 (a)). Given that the friction models were constructed without using the direct cylinder force measurement, the PID controller used as the benchmark was completely implemented under indirect force measurement.

$$u_{PID} = K_P e(t) + K_I \int e(t)dt + K_D \frac{de(t)}{dt} \quad (8)$$

4.2 Friction compensated fuzzy controller

The proposed fuzzy control system used in this study were designed as two fuzzy control modules connected in series (Fig. 11). The first fuzzy control module took care of the friction compensation. The input to the first fuzzy module were estimated friction and feedback tracking error, and its output was modified error. This first fuzzy control module acted in a similar way to the friction compensation of the desired force command utilized in the PID controller. It was experimentally tuned so that its modified error output was larger than its feedback tracking error in some certain events especially at the beginning of the direction-changing motion. This gave an extra compensation for the inaccuracy of the friction estimation that the PID controller lacked. For the PID controller, only PID gains were to be experimentally tuned.

The task of the second fuzzy control module was to calculate the control action to the EHS. Its input included modified error received from the first fuzzy module and feedback force error difference. This second fuzzy control module replicated the conventional

Received: July 6, 2022. Revised: July 30, 2022.

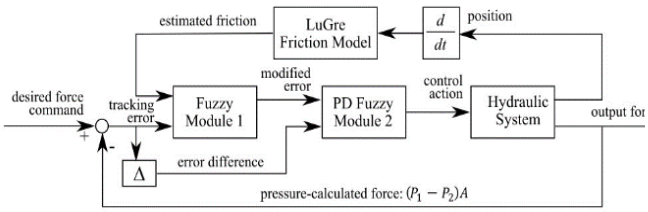

Figure. 11 Fuzzy control with friction compensation block diagram

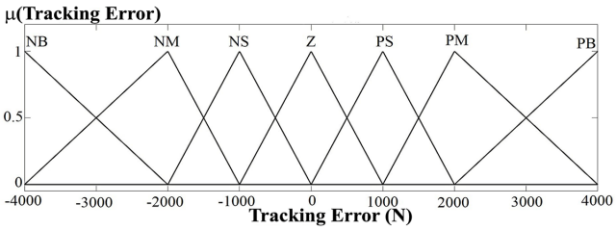

(a)

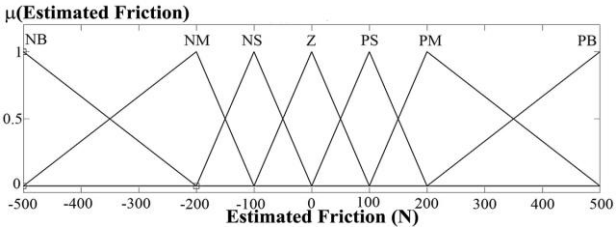

(b)

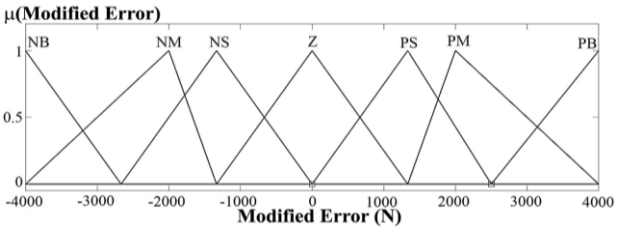

(c)

Figure. 12 Membership functions of fuzzy Control module 1: (a) tracking error input, (b) estimated friction input and (c) modified error output

PD control scheme. Various membership functions were tested for their effectiveness in the applications of obstacle climbing robot speed control [22] and antenna azimuth position control [23]. Triangular and trapezoidal membership functions gave similar transient performances, while triangular function gave the best steady state performance comparing among all the functions tested. Triangular membership functions were then used in the fuzzification stages of all inputs of both fuzzy control modules. Seven linguistic values (NB, NM, NS, Z, PS, PM, and PB) were used to interpret the values of inputs and outputs of both fuzzy modules. The letters N, Z and P denote negative, zero and positive; whereas the letters B, M and S denote big, medium and small, respectively. Figs. 12 and 13 show the membership functions of the first and second fuzzy

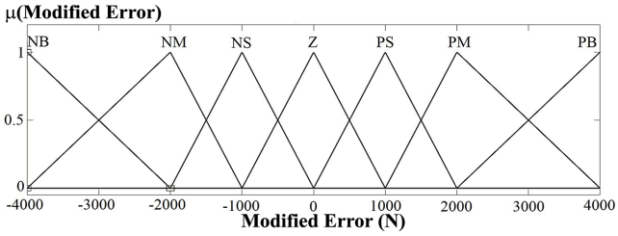

(a)

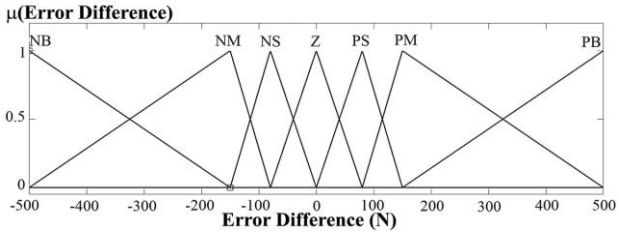

(b)

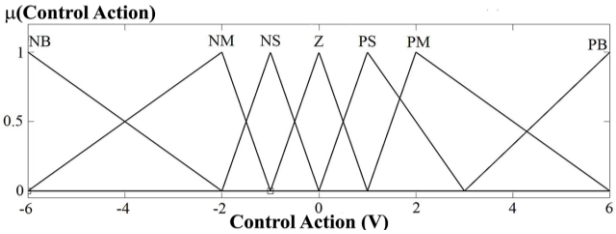

(c)

Figure. 13 Membership functions of fuzzy Control module 2: (a) modified error input, (b) error difference input and (c) control action output.

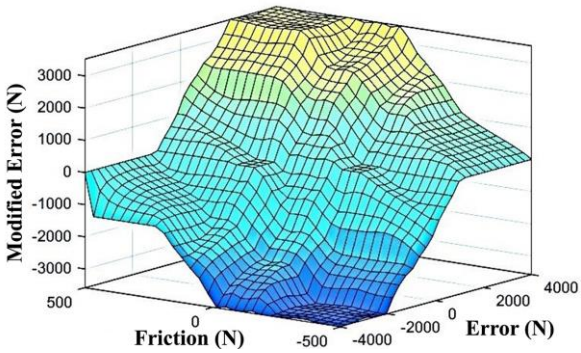

(a)

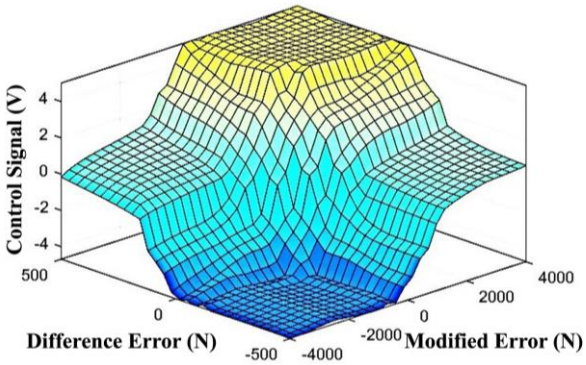

(b)

Figure. 14 Surface plots representing input-output relationships of (a) fuzzy control model 1 and (b) fuzzy control model 2

Received: July 6, 2022. Revised: July 30, 2022.

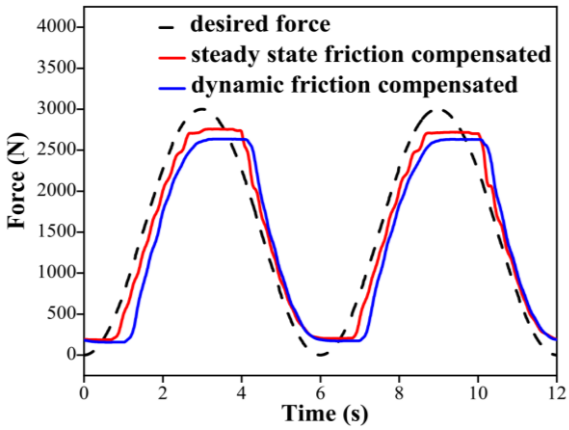

(a)

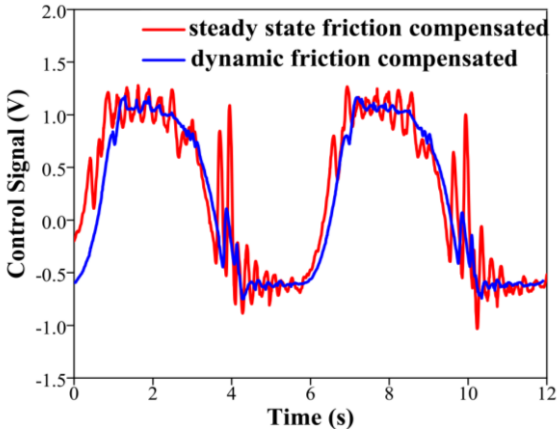

(b)

Figure. 15 Tracking performance of friction compensated PID controller on sinusoidal force command: (a) force tracking and (b) control action

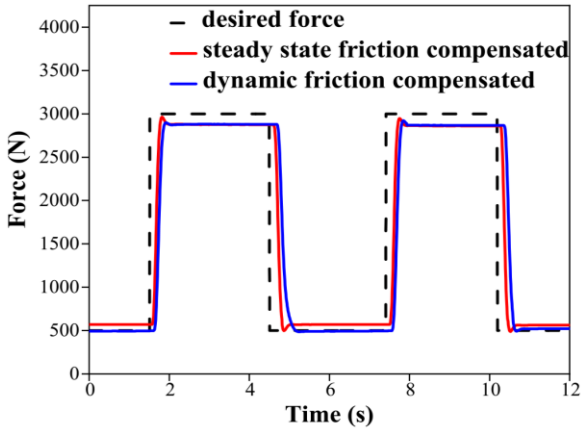

(a)

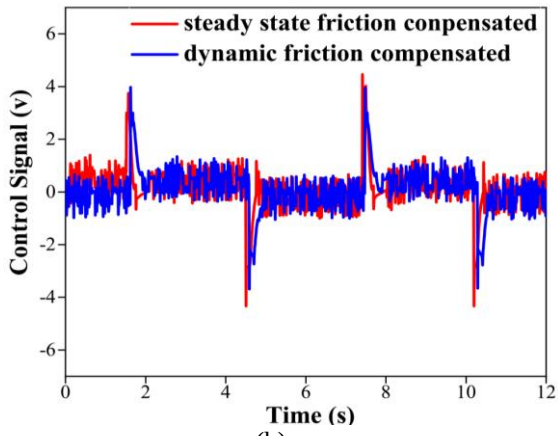

(b)

Figure. 16 Tracking performance of friction compensated PID controller on square wave force command: (a) force tracking and (b) control action

modules. The output of each rule was analyzed by the Mamdani min-max inference method. Various defuzzification methods were tested and compared [19]. It was found that the centroid of area method gave the least steady state error [19]. The centroid of area methods was then used in the defuzzification stages of both fuzzy modules. Although the rules of both fuzzy modules are not shown, their surface plots representing input-output relationships are shown in Fig. 14. Both fuzzy modules were tuned with the use of direct measured cylinder force, therefore better tracking performance of the fuzzy controller compared to the PID controller could be anticipated. Once tuning was done, the fuzzy controller was implemented with indirect pressure-calculated feedback force signal.

5. Experimental results

Tracking performances of friction compensated PID and fuzzy control systems were verified with the use of sinusoidal and square wave force commands. Both commands had periods of 6 seconds with the lowest and highest forces of 300 and 3000, respectively. Compensations of frictions estimated by steady state and dynamic LuGre models were added to both controllers.

5.1 Friction compensated PID control systems.

Fig. 15 shows sinusoidal force tracking performances of both estimated steady state and dynamic frictions compensated PID controllers. Although pressure-calculated force was used as the force feedback signal, it is not shown on the plot. Only actual force measured by load cell is shown in the result figure. Delay could be observed at the beginning of the motion of both PID control systems (Fig. 15 (a)). Steady state friction model could estimate stiction friction immediately at small velocity closed to zero, while dynamic friction model had to be integrated from zero initial condition to obtain the friction value. This caused the larger delay in the control action of the dynamic friction compensated system (Fig.15 (b)), and in tracking response (Fig. 15 (a)). The tracking errors at the

Received: July 6, 2022. Revised: July 30, 2022.

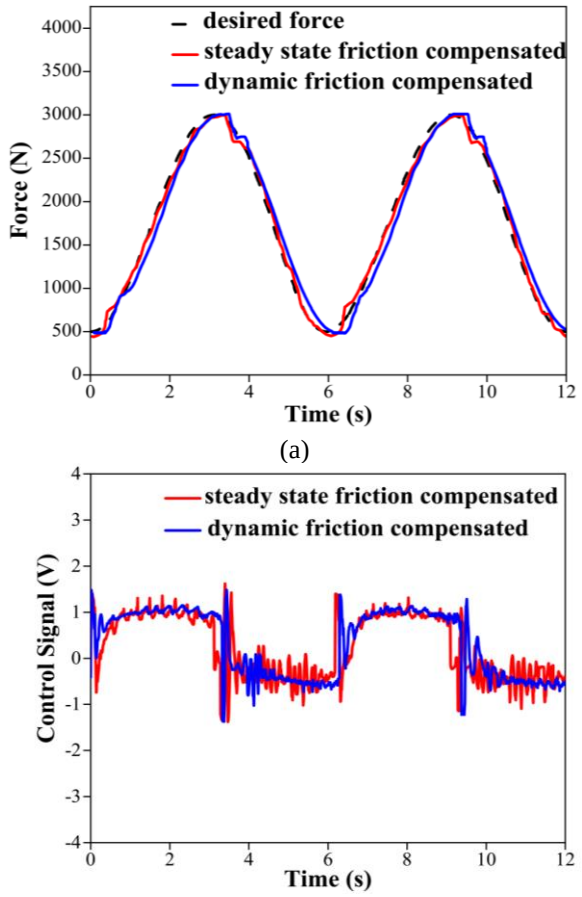

Figure. 17 Tracking performance of friction compensated fuzzy controller on sinusoidal force command: (a) force tracking and (b) control action

maximum force command of steady state friction and dynamic friction compensated controllers were 132.25 N and 230.41 N, respectively; and their RMS tracking errors were 208.41 N and 363.00 N, respectively. The static friction compensated controller gave a better tracking performance in terms of error. The control action of the dynamic friction compensated controller was smoother, and resulted in a smoother tracking.

Fig. 16 shows the square wave force tracking performances of both PID control systems. Steady state friction compensated system accomplished the tracking error at maximum compression of 119.50 N, and its RMS error was 574.87 N. As seen in the sinusoidal force tracking, larger delay at the beginning of motion could be observed on the dynamic friction compensated system. This resulted in a larger RMS error of 707.64 N, while its tracking error at maximum compression was 129.94 N. Control action of the dynamic friction compensated system was slightly delayed compared to one of the steady state friction compensated system (Fig. 16 (b)). The PID controller already performed at its best. Had the PID gains been tuned to be more aggressive, the fluctuation in tracking would occur. The performance of the friction compensated PID control system was limited by the accuracy of the friction estimation. The tracking error was due to the inaccuracy of the friction estimation.

5.2 Friction compensated fuzzy control systems

Fig. 17 shows sinusoidal force tracking performances of steady state friction and dynamic friction compensated fuzzy controllers. Similar performances could be observed for both controllers. As seen in the tests of PID cases, the control action (Fig. 17 (b)) and force tracking (Fig. 17 (a)) of the dynamic friction compensated system is slightly delayed when compared to the steady state friction compensated system. The tracking errors at the maximum force command of the steady state friction and dynamic friction compensated fuzzy controllers were 27.24 N and 41.87 N, respectively; and their RMS errors were 66.79 and 169.01, respectively. Fuzzy controllers whether with compensation of steady state friction or dynamic friction yielded superior tracking performance to the PID controller. The first fuzzy control module was tuned in experiments so that it gave modified error output larger than its feedback tracking error input at the beginning of direction-changing motion. This resulted in more aggressive control actions at the beginning of direction-changing motion of the fuzzy controllers (Fig. 17 (b)) compared to ones of the PID controllers (Fig. 15 (b)). Had the estimated friction be compensated by adding to the desired force command and the fuzzy controller was tuned without using direct cylinder force measurement, the same way as done in the PID controller, fuzzy controllers would yield similar tracking performances to the PID controllers.

Tracking performances to the square wave force command of the steady state friction and dynamic friction compensated fuzzy controllers are shown in Fig. 18. Steady state friction compensated system yielded the tracking error the maximum compression of 29.42 N and the RMS error of 439.26 N. Like all the tests previously explained, dynamic friction compensated system gave a slightly delayed tracking. Its tracking error at the maximum compression and RMS error were 34.18 N and of 486.43 N, respectively.The control actions of both fuzzy controllers were hold at their maximum values in time intervals longer than the PID controllers. The friction compensated fuzzy controller outperform the friction compensated PID controller in all conducted tests. Unlike the PID controller that its performance depends on the accuracy of friction estimation, the

Received: July 6, 2022. Revised: July 30, 2022.

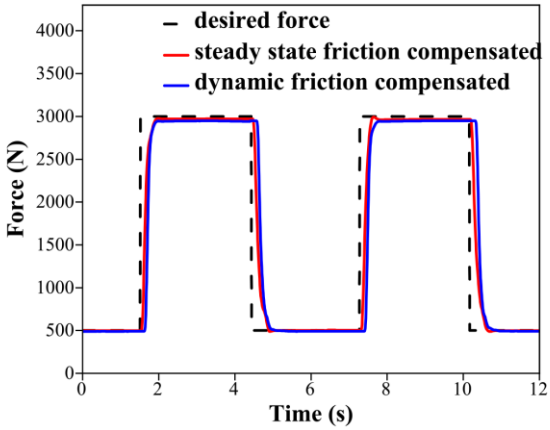

(a)

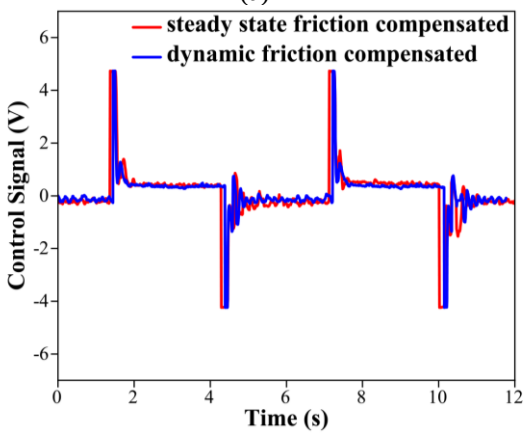

(b)

Figure. 18 Tracking performance of friction compensated fuzzy controller on square wave force command: (a) force tracking and (b) control action

Table 3. Summary of the tracking performances achieved by friction compensated PID and Fuzzy controllers

Control system	Desired force	Friction model	RMS Error (N)	F_{max} Error (N)
PID	sine	steady st.	208.41	132.25
	sine	dynamic	363.00	230.41
	square	steady st.	574.87	119.50
	square	dynamic	707.64	129.94
Fuzzy	sine	steady st.	66.79	27.24
	sine	dynamic	169.01	41.87
	square	steady st.	439.26	29.42
	square	dynamic	486.43	34.18

fuzzy controller could be experimentally tuned to cope with the inaccuracy of friction estimation. Table 3 shows the summary of the force tracking performance achieved by both friction compensated PID and fuzzy controllers.

6. Conclusions

This study presented the tracking performance comparison of the friction compensated PID and fuzzy electro-hydraulic control systems. Instead of using the actual cylinder force, both control systems used pressure-calculated force as the feedback force signal. Steady state and dynamic LuGre friction models of the EHS cylinder system were experimentally constructed with only the indirect pressure-calculated cylinder force. Sinusoidal and square wave forces with the values varying between 500-3,000 N were used as desired commands in the performance tests. The conclusions of the study are as follows.

1. The friction estimated with the steady state LuGre model was noisy compared to the dynamic model especially when estimating around the zero velocity, hence its control action was always noisier. Longer delay in control action and tracking was observed from the dynamic friction compensated control system.

2. Friction compensation is essential for a precise force control system. Without friction compensation, the sinusoidal force tracking error at the 3,000 N maximum force command of the PID controller was 500.71 N. With friction compensation, the tracking errors at the maximum command of the completely indirect PID force controllers were reduced to lowest values of 132.25 N. The tracking errors at the maximum command were reduced to lowest values of 27.24 N for the fuzzy controllers.

3. Compensation of the steady state friction is easier to implement in real world applications than the dynamic friction because it implements like a table lookup and does not require integration. The steady state friction compensation also accomplished better tracking performances in all conducted tests no matter what type of controller was.

4. Friction compensated fuzzy controllers were superior in tracking performance than the friction compensated PID controllers in all test cases due to its flexibility in friction compensation and its performance tuning with the direct measured cylinder force. The tracking performance of the friction compensated PID controllers were limited by the accuracy of friction estimation.

Conflicts of interest

The authors declare no conflict of interest.

Author contributions

Weerapong Chanbua designed and carried out the experiments, collected the data, analyzed the results and prepared the manuscript. Unnat Pinsopon verified the design, experiments analysis, and edited the manuscript.

Notations

z	The average deflection of bristles
ν	The relative velocity of the two surface
α_0	The bristle stiffness
F_c	The Coulomb friction
F_s	The stiction friction
ν_s	The Stribeck velocity
α_1	The damping coefficient of the bristle
α_2	The viscous damping coefficient of the surface contact
z_{ss}	The bristle steady state deflection
F_{ss}	The steady state friction
$F_{friction}$	Friction force
P_1	The oil pressure at the oil-incoming cylinder end
P_2	The oil pressure at the oil-incoming cylinder end
A	Piston area
m	Piston mass
a	Piston acceleration
u_{PID}	The PID control action
K_p	The gain for the proportional
K_I	The gain for the integral
K_D	The gain for the derivative

References

[1] H. M. Chen, G. W. Yang, and C. C. Liao, "Precision Force Control for an Electro-Hydraulic Press Machine", *Smart Science*, Vol. 2, No. 3, pp. 132-138, 2014.

[2] J. A. L. Pérez, E. R. D. Pieri, and V. J. D. Negri, "Force Control of Hydraulic Actuators using Additional Hydraulic Compliance", *Journal of Mechanical Engineering*, Vol. 64, pp. 579-589, 2018.

[3] H. B. Yaun, H. C. Na, and Y. B. Kim, "Robust MPC-PIC Force Control for an Electro-Hydraulic Servo System with Pure Compressive Elastic Load", *Control Engineering Practice*, Vol. 79, pp. 170-184, 2018.

[4] M. E. S. M. Essa, M. A. S. Aboelela, M. A. M. Hassan, and S. M. Abdrabbo, "Model Predictive Force Control of Hardware Implementation for Electro-Hydraulic Servo Syste", *Transactions of the Institute of Measurement and Control*, Vol. 41, No. 5, pp. 1435-1446, 2019.

[5] B. Yu, R. Liu, Q. Zhu, Z. Huang, Z. Jin, and X. Wang, "High-Accracy Force Control with Nonlinear Feedforward Compensation for a Hydraulic Drive Unit", *IEEE Access*, Vol. 7, pp. 101063-101072, 2019.

[6] S. W. Kim, B. Cho, S. Shin, J. H. Oh, J. Hwangbo, and H. W. Park, "Force Control of a Hydraulic Actuator with a Neural Network Inverse Model", *IEEE Access*, Vol. 6, No. 2, pp. 2814-2821, 2021.

[7] K. Inoue, T. Yoneda, and S. Hyon, "Joint Torque Control by Pressure Feedback on Hydraulic Excavator for Robotic Application", In: *Proc. of the 9th JFPS International Symposium on Fluid Power*, Matsue, Japan, pp. 297-304, 2014.

[8] A. Grimmert, and P. Wiederkehr, "Indirect Force Measurement using Spindle Currents for Grinding Process in Aerospace Industry", In: *Proc. of the Machining Innovations Conference for Aerospace Industry (MIC) 2021*, Hannover, Germany, pp. 082-088, 2021.

[9] H. Mostaghimi, C. I. Park, G. Kang, S. S. Park, and D. Y. Lee, "Reconstruction of Cutting Force through Fusion of Accelerometer and Spindle Current Signals", *Journal of Manufacturing Processes*, Vol. 98, pp. 990-1003, 2021.

[10] B. Denkena, B. Bergmann, and D. Stoppel, "Reconstruction of Process Force in a Five-Axis Milling Center with a LSTM Neural Network in Comparison to a Model-Based Approach", *Journal of Manufacturing and Materials Processing*, Vol. 4, No. 62, pp. 1-13, 2020.

[11] H. Feng, W. Qiao, C. Yin, H. Yu, and D. Cao, "Identication and Compensation of Non-Linear Friction for a Electro-Hydraulic System", *Mechanism and Machine Theory*, Vol. 141, pp. 1-13, 2019.

[12] K. Umeda, T. Sakuma, K. Tsuda, and S. Sakaino, "Reaction Force Estimation of Electro-Hydrostatic Actuator using Reaction Force Observer", *IEEJ Journal of Industry Applications*, Vol. 7, No. 3, pp. 250-258, 2018.

[13] P. Zeng, G. Jiang, C. Zou, X. Zhang, and C. Xie, "Nonlinear Friction Compensation of a Flexible Robotic Joint with Harmonic Drive", *Applied Mechanics and Materials*, Vol. 868, pp. 39-44, 2017.

[14] Y. H. Sun, T. Chen, C. Q. Wu, and C. Shafai, "Comparison of Four Friction Models: Feature Prediction", *Journal of Computational and Nonlinear Dynamics*, Vol. 11, No. 3, pp. 1-10, 2015.

[15] C. S. Huang, S. S. Yeh, and P. L. Hsu, "Estimation and Compensation of the LuGre Friction Model in High-Speed Micro-Motion Control", *International Journal of Automation and Smart Technology*, Vol. 7, No. 3, pp. 101-109, 2017.

[16] X. B. Tran, "Nonlinear Control of a Pneumatic Actuator Based on a Dynamic Friction Model", *Journal of Mechanical Engineering*, Vol. 67, No. 9, pp. 458-472, 2021.

[17] S. Jiang, K. Zhang, H. Wang, D. Zhong, J. Su, and Z. Liu, "Research on Adaptive Friction Compensation of Digital Hydraulic Cylinder Based on LGre Friction Model", *Shock and Vibration*, Vol. 21, pp. 1-10, 2021.

[18] Y. S. Awood, A. K. Mahmood, and M. A. Ibrahim, "Comparison of PID, GA and Fuzzy Loic Controllers for Cruise Control System", *International Journal of Computing and Digital Systems*, Vol. 7, No. 5, pp. 311-319, 2018.

[19] A. Kharidege, D. Jianbiao, and Y. Zhang, "Performance Study of PID and Fuzzy Controllers for Position Control of 6 DOF arm Manipulator with Various Defuzzification Strategies", In: *Proc. of ICMMR 2016 MATEC Web of Conf.*, Chongqing, China, Vol. 77, pp. 1-6, 2016.

[20] Y. Y. Lai and K. M. Chang, "Fuzzy Control for a Pneumatic Positioning System", In: *2017 9th International Conference on Modelling, Identification and Control (ICMIC)*, Kunming, China, pp. 231-236, 2017.

[21] H. Olsson, K. J. Asrom, C. C. D. Wit, M. Gafvert, and P. Lischinsky, "Friction Models and Friction Compensation", *European Journal of Control*, Vol. 4, No. 3, pp. 176-195, 1998.

[22] K. A. Malik, D. Elayaraja, S. J. A. Ibrahim, and N. S. K. Chakravarthy, "Investigating the Potential Consequences of the Membership Functions in a Fuzzy Logic Controller-Based Obstacle Climbing Robot", *IT in Industry*, Vol. 9, No. 1, pp. 1294-1299, 2021.

[23] O. A. M. Ali, A. Y. Ali, and B. S. Sumait, "Comparison between the Effects of Different Types of Membership Functions on Fuzzy Logic Controller Performance", *International Journal of Emerging Engineering Research and Technology*, Vol. 3, No. 3, pp. 76-83, 2015.